Chemical Engineering Journal 151 (2009) 51–58

Contents lists available at ScienceDirect

Chemical Engineering Journal

journal homepage: www.elsevier.com/locate/cej

A combined photocatalytic and electrochemical treatment of wastewater containing propylene glycol methyl ether and metal ions

H.D. Doan [a,*], A. Weli [b], J. Wu [a]

[a] Department of Chemical Engineering, Ryerson University, 350 Victoria St., Toronto, Ontario, Canada M5B 2K3
[b] Rio Tinto Alcan, Kitimat, British Columbia, Canada

ARTICLE INFO

Article history:
Received 4 November 2008
Received in revised form 19 January 2009
Accepted 26 January 2009

Keywords:
PGME
Nickel
Zinc
Photocatalysis
Electrodeposition

ABSTRACT

Simulated wastewater containing Ni^{2+}, Zn^{2+} and propylene glycol methyl ether (PGME), a solvent in polymer solution used in metal coating, was treated by a combined electrochemical and photocatalytic technique. The effect of electrode spacing and corrugated electrodes on the removal of Ni^{2+} and Zn^{2+} by electrodeposition was investigated. The solution pH and temperature were kept at 6.0 and 25 °C. The metal removal was almost doubled when the electrode spacing was decreased from 6.4 to 1.3 cm. A further 40% increase was obtained with the corrugated cathode at the electrode spacing of 1.3 cm. A 96% removal of Ni^{2+} and Zn^{2+} was obtained after 48 h of treatment at a liquid flux of 0.0334 $m^3\ m^{-2}\ s^{-1}$.

For the combined electrochemical–photocatalytic treatment in a rotary reactor, using immobilized TiO_2 at a liquid flux of 0.0148 $m^3\ m^{-2}\ s^{-1}$, metal concentrations decreased about 35% after 48 h of treatment. Lower metal removal could be attributed to the lower liquid flux and the higher liquid volume of 2.4 times that used in the sole electrochemical treatment. However, the PGME removal of 6.9 mg cm^{-2} was obtained. This was much higher than the removal amounts of 4.5 mg cm^{-2} and 1.9 mg cm^{-2} for the sole photocatalytic method and the sole electrochemical treatment, respectively.

1. Introduction

New development in a variety of industrial fields to meet increasing requirements of human consumption has led to the disposal of numerous toxic compounds in the effluent streams, which are not readily degraded by the conventional effluent treatment methods [1–3]. Industrial wastewater contributes to about 42% of the total volume of wastewater in the world. In the metal finishing industry, various coating processes are used to provide protective coating on metal parts. Specifically, electro-coating is often used for aluminum and steel parts and car frames in automotive industry. The coating process usually starts with a washing step that involves a two-stage cleaning of metal parts with an alkaline solution and rinsing them with water. Once the metal parts have been washed, they are sent to a phosphate anti-corrosive pretreatment with water post-rinse, coated with a protective polymer layer and rinsed with de-ionized water before being cured at high temperature. Therefore, the coating process generates a large amount of wastewater. The paint (polymer solution) used in electro-coating contains pigment, resin, de-ionized water, and other additives. These additives include coalescing solvents such as propylene glycol methyl ether (PGME). Coalescing agents improve the quality of the resin film formation on metal parts. The rinse water from the coating process contains Zn^{2+}, Ni^{2+} at a typical concentration of 20 ppm each and organic compounds, mainly PGME at about 200 ppm [4]. Therefore, in the present study Zn^{2+}, Ni^{2+} and PGME were chosen as model components in the simulated wastewater.

Many methods have been used for the treatment of industrial wastewater. They include filtration, settling ponds, biological oxidation, electro-flotation, electro-winning and chemical precipitation. The most commonly used method for inorganic pollutants is chemical precipitation, especially in mining and metal finishing industries. However, chemical precipitation generates sludge that contains high concentrations of heavy metals and needs be disposed off as a hazardous material [5].

Electrodeposition of metals from aqueous solution is an attractive alternative for the recovery of metal ions from industrial effluents such as those from plating, metal finishing, and electronic industries. Electrochemical recovery of heavy metals from rinse water is of interest because pure metals may be recovered for recycling without sludge generation. The main advantage of the electrochemical process is that it is an environmentally friendly process, since it does not require addition of chemicals.

Advanced oxidation processes (AOPs) are effective remediation and treatment methods due to their ability to completely degrade a wide variety of organic pollutants that are not readily degradable by conventional wastewater treating methods. TiO_2 induced photocatalysis is an established AOP for the treatment of contam-

* Corresponding author. Tel.: +1 416 979 5000x6341; fax: +1 416 979 5083.
E-mail address: hdoan@ryerson.ca (H.D. Doan).

1385-8947/$ – see front matter © 2009 Elsevier B.V. All rights reserved.
doi:10.1016/j.cej.2009.01.041

Nomenclature

A	electrode area (m^2)
C	concentration at a given time ($mg\,L^{-1}$)
C_0	initial concentration ($mg\,L^{-1}$)
C_S	concentration of metal ions at the surface of the cathode ($mg\,L^{-1}$)
d	distance between the cathode and the anode in the electro-cell, 0.013 m
D_{AB}	diffusivity of metal ions in liquid ($m^2\,s^{-1}$)
E°	standard half-cell potential (V)
H	the depth of the liquid in the electro-cell, 0.10 m
k	rate constant for first-order kinetics of metal removal (h^{-1})]
k_c	mass transfer coefficient for metal ions ($m\,h^{-1}$)
L	characteristic length (hydraulic diameter of the opened-channel electro-cell in the present study) ($L = \{4dH/2(d+H)\}$) (m)
$[Ni^{2+}]_0$	initial Ni^{2+} concentration ($mg\,L^{-1}$)
$[PGME]_0$	initial PGME concentration ($mg\,L^{-1}$)
r	rate of metal removal in the electro-cell ($mg\,L^{-1}\,h^{-1}$)
Re	the Reynolds number ($Re = [L\rho u]/\mu$)
r_m	rate of mass transfer of metal ions from liquid to the cathode ($mg\,h^{-1}$)
Sh	the Sherwood number ($Sh = [k_c L]/D_{AB}$)
Sc	the Schmidt number ($Sc = \mu/[\rho D_{AB}]$)
t	time (h)
u	superficial liquid velocity ($m\,s^{-1}$)
V	liquid volume (m^3)
$[Zn^{2+}]_0$	initial Zn^{2+} concentration ($mg\,L^{-1}$)

Greek symbols

ρ	liquid density ($kg\,m^{-3}$)
μ	liquid viscosity ($kg\,m^{-1}\,s^{-1}$)

inated air and water streams. The capability of the photocatalytic process to completely mineralize pollutants is its great advantage over other methods.

Although the electrochemical treatment is quite effective in removing heavy metals, it is less effective in treating organic pollutants. In the same token, the photocatalytic process can degrade organic materials effectively but it has a limited effect on the removal of heavy metals. From an industrial point of view, the development of a method that could treat both heavy metals and organic pollutants concurrently is highly desirable. Therefore, the objective of the present study was to investigate the feasibility of a combined electrochemical and photocatalytic method to treat simulated wastewater containing Zn^{2+}, Ni^{2+} and PGME. In addition, the major drawback of the suspended TiO_2 process is the need of recovery of TiO_2 particles in the treated effluent by filtration, which would be tedious and costly; hence, investigation of the immobilization of TiO_2 on a solid support was also attempted in the present study.

2. Experimental method

2.1. Immobilization of TiO_2 on ceramic tiles

Two types of titanium dioxides, Degussa P25 TiO_2 and TPX-220, were used. Degussa P25 TiO_2 (Stochem Company, Toronto, Canada) is a powder containing mainly anatase. It has a surface area of $55\,m^2\,g^{-1}$. Degussa P25 TiO_2 was used as a photocatalyst in a suspended form. TPX-220 (Green Millennium, California, USA) is a mixture of peroxo-titanium acid solution and peroxo-modified anatase solution. The average particle size of TPX-220 was 10 nm.

Square ceramic tiles, 10.2 cm × 10.2 cm, were used as a support base on which TiO_2 was immobilized. The immobilization of TiO_2 on a ceramic tile was done by spraying a thin layer of the TiO_2 solution (TPX-220) to cover the whole surface of the tile. The TiO_2 coated tile was left to dry at room temperature for 24 h. The tile was then heated to 600 °C for 5 h and allowed to cool down to room temperature before being used in the experiments. Other curing temperatures of 25, 150, 300 and 650 °C were also tested. All cured ceramic tiles coated with a very thin layer of TiO_2 were rinsed with distilled water to remove loose TiO_2 particles before used. It was thus rather difficult to determine the exact amount of TiO_2 on the ceramic tile. By visual observation, the surface of the TiO_2 coated ceramic tile appeared to be smooth with a dull look. Therefore, the nominal surface area of the ceramic tile was used in the calculation of the PGME removal per unit area of TiO_2.

2.2. Experimental set-up

2.2.1. Sole electrochemical process

The experimental set-up consisted of a PVC rectangular open channel as shown in Fig. 1. The open channel (100 cm long, 7.5 cm wide and 20 cm high) along with the stainless steel anodes and aluminum cathode formed an electro-cell. Liquid was recirculated through the electro-cell from a holding tank containing 50 L of simulated wastewater. A cooling coil and an automatic controlled heater were installed in the tank to maintain the liquid temperature at 25 °C. A flow meter (Model F-45750-LHN12, Fabco Co., Maple, Ontario) was used to monitor the liquid flow rate. Initial concentrations of Zn^{2+} and Ni^{2+} were 20 ppm each. In addition, 500 ppm of potassium sulfate was used in all experiments as a supporting electrolyte.

Two stainless steel anodes and one aluminum cathode, each of 19.0 cm long and 10 cm immersed in liquid were used in all experimental runs. The cathode and anodes were connected to the negative and positive terminals of a DC power supply, respectively. An amp-meter was connected in series in the circuit to measure the electric current through the electrodes. In order to have an even flow of liquid in the channel, the liquid inlet stream was spread out using a liquid distributor placed at the bottom of the electro-cell. To investigate the effect of electrode spacing on the metal removal, the distance between the anode and the cathode was varied over a range of 1.3–6.4 cm. The liquid flow rate was set at $0.0334\,m^3\,m^2\,s^{-1}$.

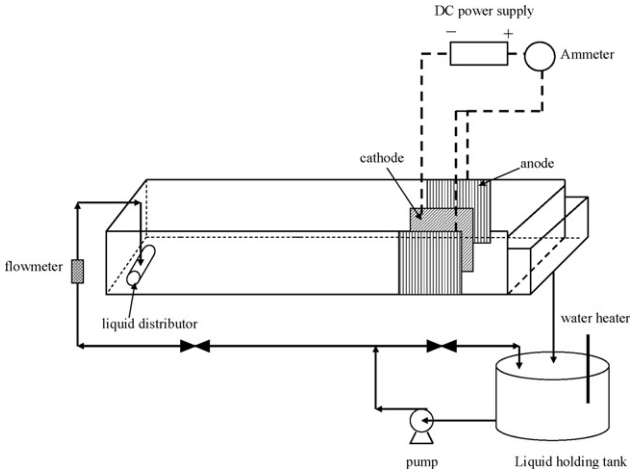

Fig. 1. Experimental set-up for the sole electrochemical treatment.

For the investigation of the effect of the electrode configuration on the metal removal, a corrugated aluminum cathode was used in the same experiments set-up with flat stainless steel anodes. To fabricate the corrugated electrode, a flat aluminum plate (the same size of the flat electrode, 19 cm × 15 cm) was bent into segments of 0.50 cm long at 90° angles one to another.

2.2.2. Sole photocatalytic process in a batch system

A batch system was used for the preliminary test of the removal of PGME by suspended and immobilized TiO_2. The experimental set-up consisted of a glass container, a UV lamp and a magnetic stirrer. This set-up was also used to test the effect of the curing temperature and the curing time of the TiO_2 immobilization on the removal of PGME. For experiments with suspended TiO_2, 0.015 g of Degussa P25 TiO_2 powder was added to 1 L of a 200 ppm PGME solution in the glass container. The solution had been allowed to mix by the magnetic stirrer for 1 h before the 254 nm UV lamp (model UVS-28, 115 V, 0.31 Amp, UPV, Upland, California, USA) was turned on. Water samples were then collected continually at preset intervals and analyzed for the PGME concentration using a gas chromatograph (PerkinElmer auto system XL, MA, USA). The same procedure was used for experiments with the TiO_2 coated ceramic tile.

2.2.3. Combined electrochemical and photocatalytic treatment in a rotary reactor

A rotary reactor was used for this stage of the present study. A sketch of the experimental set-up is given in Fig. 2. A holding tank contained 120 L of simulated wastewater, which was pumped to a rotary photocatalytic reactor and then passed through an electro-cell before returning to the liquid holding tank. The electro-cell was made of PVC with the dimensions of 50 cm long × 30 cm wide × 17 cm high. The photocatalytic reactor had two 25-cm-diameter PVC disks that were mounted on a rotating shaft at the center of the disks. The disks were rotated at 10 rpm (equivalent disk peripheral velocity of 13.2 cm s^{-1}). The disks held six ceramic tiles coated with TiO_2 on the outside surface.

In order to evaluate the direct photochemical oxidation of PGME by the UV light, a blank experiment without TiO_2 was carried out in the rotary reactor at a liquid flux of 0.0148 m^3 m^{-2} s^{-1}. There was no significant degradation of PGME by the UV light only. In addition, a photocatalytic experiment (without an electro-cell) was conducted using a solution containing 20 ppm each of Zn^{2+} and Ni^{2+}. The results obtained did not show any significant reduction in the metal ion concentration.

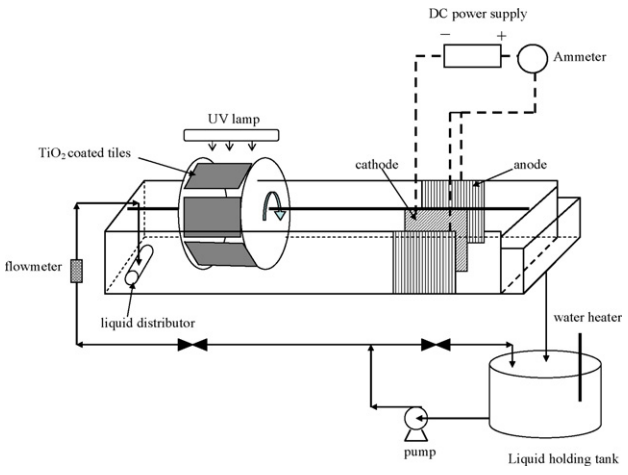

Fig. 2. Experimental set-up for the combined electrochemical and photocatalytic method.

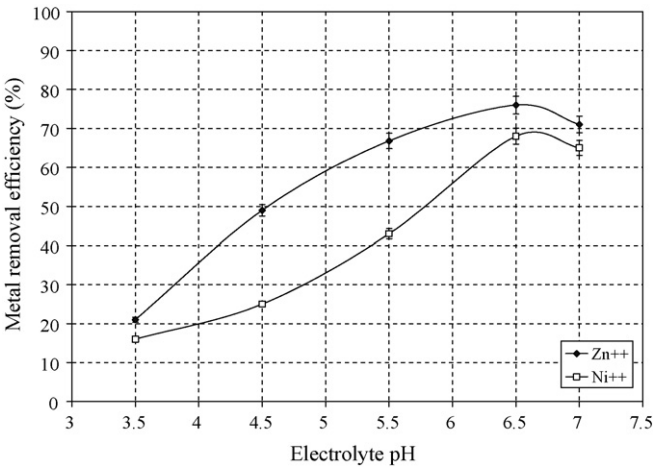

Fig. 3. Effect of electrolyte pH on the metal removal, 48 h of treatment, applied voltage = 4 V, $[Zn^{2+}]_0 = [Ni^{2+}]_0 = 20$ ppm, $[K_2SO_4]_0 = 500$ ppm, $T = 25$ °C, pH 6.0, liquid flux = 0.0334 m^3 m^{-2} s^{-1}.

3. Results and discussion

3.1. Sole electrochemical deposition of metal ions

3.1.1. Effect of electrolyte pH on metal deposition

Many factors affect the removal of metal ions in an electrochemical cell. One of the crucial factors is the electrolyte pH. It was indeed the case as observed in the present study. For both Ni^{2+} and Zn^{2+}, the metal deposition increased with the electrolyte pH over a range from 3.5 to 6.5, and decreased slightly at pH of 7.0, as can be seen in Fig. 3. At the initial pH of 7.0, some metal precipitate was found in the experimental apparatus. This may be attributed to the decrease in the metal deposition at pH of 7.0. It was also noted that the removal of Zn^{2+} was consistently higher than that of Ni^{2+}. At a low pH, there would be more competition for electrons at the cathode surface by H^+ in the electrolyte, resulting in fewer electrons available for the metal deposition; hence, a lower metal removal was observed. The removal of Zn^{2+} increased sharply at pH of 3.5–4.5 while Ni^{2+} removal increased more rapidly at pH from 5.5 to 6.5. However, it has been reported in the literature that for nickel deposition from rinse water of plating baths, the highest rate of nickel recovery was at the bulk pH of 5.4–5.6 [6]. Perhaps, the presence of other components in the plating rinse water affected the deposition of nickel.

It was also noted that the electrolyte pH changed during an experiment. In order to understand the change of the electrolyte pH during the course of the experiment, several electrode reactions may be considered as following [7,8]:

1. Metals deposition at the cathode:

$$Zn^{2+}(aq) + 2e^- \leftrightarrow Zn(s) \quad E^\circ = -0.76\,V$$

$$Ni^{2+}(aq) + 2e^- \leftrightarrow Ni(s) \quad E^\circ = -0.23\,V$$

2. Side reactions at the cathode such as hydrogen evolution, water hydrolysis and oxygen reduction:

$$2H^+ + 2e^- \leftrightarrow H_2 \quad E^\circ = 0.0\,V \tag{R.1}$$

$$2H_2O + 2e^- \leftrightarrow H_2 + 2OH^- \quad E^\circ = -0.83\,V \tag{R.2}$$

$$O_2 + 4H^+ + 4e^- \leftrightarrow 2H_2O \quad E^\circ = +1.23\,V \tag{R.3}$$

3. Water decomposition at the anode:

$$H_2O \leftrightarrow 1/2O_2 + 2H^+ + 2e^- \quad E^\circ = -1.23\,V \qquad (R.4)$$

In the present study, it was observed that the bulk pH decreased in the first 8 h and became stable up to 24 h of treatment. However, in the following 24 h the bulk pH increased. Concentrations of Ni^{2+} and Zn^{2+} were high initially. The main reactions would thus be the reduction of metal ions at the cathode. The main side reaction was probably the water decomposition at the anode, which resulted in an increase in the electrolyte acidity. On the other hand, other H^+ consuming side reactions at the cathode (such as reactions (R.1) and (R.3)) could also take place. However, due to competition with the metal deposition at the cathode, the rates of these reactions at the cathode might be lower than that of the water decomposition at the anode. Consequently, the electrolyte pH decreased initially. After the first 24 h of treatment, the concentrations of Ni^{2+} and Zn^{2+} at the cathode decreased significantly. This would create a favorable environment for other side reactions at the cathode to take place, which consumed H^+ (reactions (R.1) and (R.3)) or produced OH^- (reaction (R.2)) leading to an increase in pH at the end of 48 h of treatment. However, reaction (R.4) at the anode produced H^+ and countered the effect of the side reactions at the cathode to some extent.

By comparing the standard reduction potentials of the side reactions with those of Ni^{2+} and Zn^{2+}, one can expect that the oxygen and hydrogen reduction would occur preferentially. However, oxygen reduction would only be significant at a low metal ion concentration [9]. The reduction of dissolved oxygen was thus significant at the cathode when the metal ion concentration was much less than 20 ppm because the solubility of oxygen was about 8 ppm in an aqueous solution at room temperature. In addition, the standard reduction potential for oxygen indicates that oxygen is a strong oxidizing agent. However, since oxygen reduction involves the transfer of four electrons and four hydrogen ions as shown in reaction (R.3), the overpotential required for this reaction is very high. This reaction is thus very slow and usually requires a catalytic electrode such as platinum [8]. In the present study no such electrode was used; thereby, the reduction of oxygen molecules would not be significant.

For H^+ reduction at the cathode, the actual potential at which the reaction occurred was much lower (more negative) than its standard potential [10]. Lead, zinc and aluminum electrodes do not adsorb hydrogen to a great extent; hence, a greater overpotential is required to achieve a significant rate of hydrogen evolution [11]. In the present study, after 24 h of treatment the concentration of metal ions was depleted substantially while the voltage across the cell was kept constant. Therefore, excess electrons were available for side reactions, such as hydrogen evolution. It is believed that the required cathode potential for the reduction of hydrogen was reached at the end of the experiment, resulting in the depletion of H^+, and hence, the observed pH rise.

Over the current density range of 0.20–0.70 mA cm^{-2} used in the present study, electrodeposition of Ni^{2+} and Zn^{2+} exhibited an anomalous co-deposition since Zn^{2+}, the less noble metal, deposited preferentially. Several researchers have studied this phenomenon and reported that the current density and the concentration of Ni^{2+} in the binary metal solution strongly influenced the composition and the morphology of the deposit [12–14]. At high current densities, water hydrolysis produced OH^- at the cathode; thereby, $Ni(OH)_2$ and $Zn(OH)_2$ were formed at the cathode rather than elemental metal deposition. $Zn(OH)_2$ precipitation and adsorption on the cathode preceded that of $Ni(OH)_2$, resulting in the anomalous co-deposition [12]. On the other hand, at a current density of 10 mA cm^{-2}, normal co-deposition of Ni^{2+} and Zn^{2+} in a chloride bath containing NH_4Cl was reported [13,14]. It is relevant to note that although the current density used in the present study was much less than that used in the reported literature for Ni^{2+} and Zn^{2+} deposition in a chloride bath, deposition anomaly of Ni^{2+} and Zn^{2+} still existed in the SO_4^{2-} solution used in the present study.

3.1.2. Electrode spacing and configuration

The effect of the electrode spacing on the removal of Ni^{2+} and Zn^{2+} was also examined. The metal removal increased from 37% to 60% and 33% to 70% for Ni^{2+} and Zn^{2+}, respectively, when the electrode spacing was decreased from 6.4 to 1.3 cm, as shown in Fig. 4. According to the Ohms law of voltage, the applied voltage is proportional to the current and the resistance of the electro-cell. At a constant applied voltage of 4.0 V, a reduction in the electrode spacing resulted in a decrease in the resistance between the anode and the cathode. Consequently, the electric current through the system increased. This led to an increase in the current density, i.e. more electrons available at the cathode for the deposition of Ni^{2+} and Zn^{2+}. This was indeed the case as can be seen by the increase in the measured current density with the reduction of the electrode spacing shown in Fig. 4.

It is relevant to note that the current density is an indication of the metal deposition process that consumes electrons at the cathode. Therefore, both the metal removal and the current density varied in the same trend with the electrode spacing. The metal removal or the current density increased gradually when the electrode spacing was reduced from 6.4 to 2.5 cm. However, a sharp increase in the current density was observed when the electrode spacing was further reduced from 2.5 to 1.3 cm. On the overall, the amount of metal removed for both Ni^{2+} and Zn^{2+} was almost doubled with the reduction of the electrode spacing from 6.4 to 1.3 cm. In addition, the co-deposition of Ni^{2+} and Zn^{2+} appeared to be at the transition from normal to anomalous co-deposition at the electrode spacing of 2.5 cm. At the electrode spacing less than 2.5 cm, the removal of Zn^{2+} was significantly higher than that of Ni^{2+} as can be seen in Fig. 4. This coincided with the sharp increase in the current density. At this electrode spacing, there was probably a surge in the water hydrolysis reaction that consumed electrons and produced OH^-. The hydroxyl ions from the water hydrolysis facilitated the deposition of Zn^{2+} in the form of $Zn(OH)_2$ at the cathode, resulting in the sharp increase in the current density and the significant increase in the anomalous deposition of Zn^{2+} preferentially over Ni^{2+} observed.

The effect of the electrode configuration on the removal of Ni^{2+} and Zn^{2+} was also tested using flat and corrugated electrodes. The electrode spacing was kept at 1.3 cm. The results obtained are plotted in Fig. 5. The corrugated electrode enhanced the metal removal

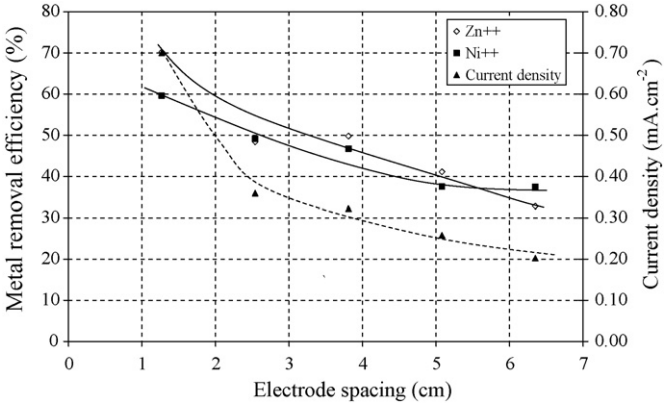

Fig. 4. Effect of electrode spacing on the metal removal, 48 h of treatment, applied voltage = 4 V, $[Zn^{2+}]_0 = [Ni^{2+}]_0 = 20$ ppm, $[K_2SO_4]_0 = 500$ ppm, $T = 25\,^\circ C$, pH 6.0, liquid flux = 0.0334 $m^3\,m^{-2}\,s^{-1}$.

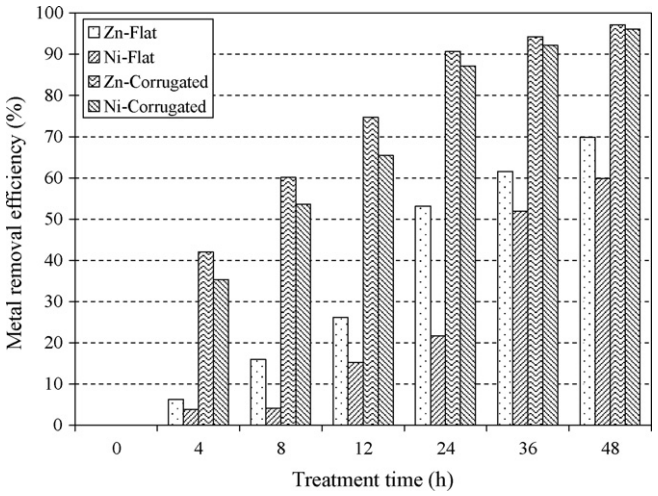

Fig. 5. Effect of the electrode configuration on the metal removal over 48 h of treatment at $T = 25\,^{\circ}C$, pH 6.0 and liquid flux of 0.0334 $m^3\,m^{-2}\,s^{-1}$.

significantly. After 4 h of treatment, the metal removal using the corrugated electrode was about 8 times that of the flat electrode. This could be due to the fact that the corrugated electrode created local turbulence that enhanced the mass transfer of the metal ions from liquid to the cathode surface. Similar mass transfer enhancement by corrugated electrodes was reported in literature [15]. However, the metal concentration exhausted with a prolonged treatment time, leading to more moderate differences between the two cases. After 48 h of treatment using the corrugated cathode as compared with the flat cathode, the metal removal increased from 60% to 96% and from 70% to 97% for Ni^{2+} and Zn^{2+}, respectively.

3.1.3. Mass transfer of metal ions in the electro-cell

In the present study, the variation of the metal concentration with the treatment time exhibited an exponential decay, indicating that the removal of metal ions followed a first-order kinetics that can be expressed as

$$r = \frac{dC}{dt} = -kC \tag{1}$$

or

$$\ln\left(\frac{C}{C_0}\right) = -kt \tag{2}$$

where C is the concentration of metal ions remaining in the solution at a given time, k is the first-order metal removal rate constant and r is the metal removal rate. As shown in Eq. (2), the values of the removal rate constant, k, can be obtained from the slopes of the semi-log plots of the normalized metal concentration (ratio of the metal concentration at a given time to the initial concentration, C/C_0) versus the treatment time, t, of the experimental data at various liquid flow rates in the present study.

The mass transfer rate of metal ions from the bulk liquid to the cathode can be written in the form of a standard rate equation as [16]:

$$r_m = k_c A(C - C_S) \tag{3}$$

where the metal ion concentration, C_S, at the cathode surface can be assumed to be zero since the metal deposition is a very fast reaction, k_c is the mass transfer coefficient and A the cathode surface area.

From Eqs. (1) and (3), the mass transfer coefficient, k_c can be obtained as below:

$$k_c = k\frac{V}{A} \tag{4}$$

where V is the volume of the electrolyte in the system.

Table 1
Physical properties of the electrolyte solution at 25 °C.

20 ppm Zn^{2+} solution	
Density[a], ρ ($kg\,m^{-3}$)	997
Viscosity[a], μ ($kg\,m^{-1}\,s^{-1}$)	0.000998
Diffusivity[b] of Zn^{2+}, D_{AB} ($m^2\,s^{-1}$)	7.02×10^{-10}

[a] Measured values using a pycnometer for density (VWR Canada, Mississauga, Ontario) and a viscometer (model V-2000 Series II, Cannon Instrument Co., PA, USA).
[b] Estimated value.

For data generalization, the dimensionless mass transfer coefficient in the form of the Sherwood number for mass transfer is often used to correlate the experimental data. It can then be used to estimate the mass transfer coefficient used in the design or performance evaluation of a large-scale system. The Sherwood number is defined as [16]:

$$\mathrm{Sh} = \frac{k_c L}{D_{AB}} \tag{5}$$

where L is the characteristic length (in the present study, it is the hydraulic diameter of the open channel electro-cell, which is 0.023 m) and D_{AB} is the diffusivity of the metal ion in liquid.

Under the conditions used in the experiments, the estimated value of D_{AB} for Zn^{2+} was $7.016 \times 10^{-10}\,m^2\,s^{-1}$ [17]. Using the experimentally determined mass transfer coefficients at various liquid flow rates from 0.0092 to 0.0277 $m^3\,m^{-2}\,s^{-1}$ (the equivalent Reynolds numbers, Re from 221 to 665), the Sherwood numbers for mass transfer of Zn^{2+} from liquid to the cathode in the electro-cell were calculated. The values of the Schmidt number, Sc for Zn^{2+} is 1425. The physical properties of the electrolyte used in the calculations of the dimensionless numbers are given in Table 1. The ratio of $Sh/Sc^{1/3}$ is plotted against the Reynolds number in Fig. 6. A correlation for the Sherwood number was then obtained by curve fitting with a good coefficient of determination, r^2, of 0.99 as can be seen in Fig. 6. For the mass transfer of Zn^{2+} from liquid to the corrugated cathode in the electro-cell, the correlation for the Sherwood number can thus be expressed as

$$\mathrm{Sh} = 2.20\,Re^{0.506}\,Sc^{1/3} \tag{6}$$

As shown in Eq. (6), the Sherwood number for mass transfer of the metal ions in the electro-cell is proportional to the Reynolds number to the power of 0.506. This is in the same order of magnitude of that for mass transfer under laminar flow over a flat plate (0.50) or in a pipe (0.33) [18]. It is also relevant to note that the constant of 2.20 in Eq. (6) is much higher than the constants of 0.33–0.85 usually found in several mass transfer correlations

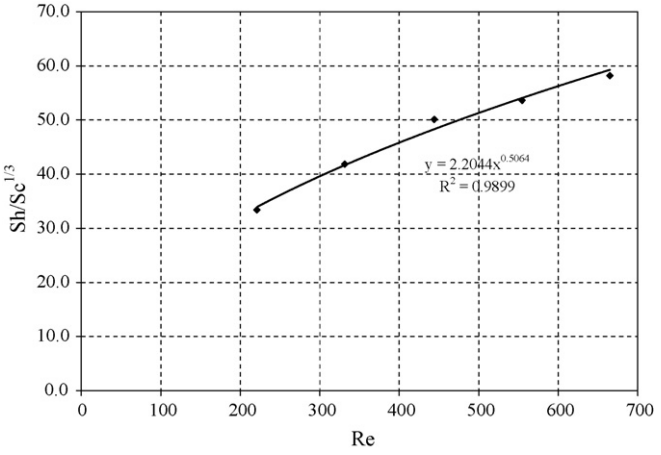

Fig. 6. Sherwood number for mass transfer of Zn^{2+} from liquid to the cathode in the electro-cell used for the sole electrochemical deposition.

for various geometries reported in literature. The higher constant for the electro-deposition of Zn^{2+} could be attributed to the mass transfer enhancement of the corrugated cathode that created local turbulence near the surface. In addition, the mass transfer coefficient obtained in the present study, using a 100-cm-long open channel for the electro-cell, appeared to be more dependent on liquid velocity than that observed in our previous study with a smaller electro-cell in a 25-cm-long open channel [19]. In the previous study, the mass transfer coefficient was found to be proportional to liquid velocity to the exponent of 0.25 as compared with the exponent of 0.506 in the present study. It is believed that with the long channel used in the present study, the entrance effect was minimized; hence, the flow was fully developed before passing the electro-cell, resulting in a higher mass transfer and a higher level of velocity dependency.

3.2. Testing in batch system

3.2.1. Effect of UV wavelength on PGME removal in a batch system

For titanium dioxide as a photocatalyst, the electron-hole can be generated if it is illuminated with a wavelength smaller than 380 nm. In the present study 3 UV lamps with wavelengths of 254, 302 and 365 nm were tested to determine the one that would give the highest PGME removal. The results obtained are presented in Fig. 7. In general, the UV light of a shorter wavelength was more effective in removing PGME, as expected, since the energy is inversely proportional to the wavelength. Since the suspended TiO_2 almost completely removed PGME using 254 nm UV light, as can be seen in Fig. 7, this light was used in all experiments thereafter.

Degussa P25 TiO_2 powder has a surface area of 55 $m^2\,g^{-1}$. Accordingly, 0.015 g of TiO_2 powder in suspension would yield a total surface area of 8250 cm^2 that was far greater than the ceramic tile surface area of 101.3 cm^2 covered with the immobilized TiO_2 layer. Therefore, although the percentage removal of PGME with the suspended TiO_2 was higher than that with the immobilized TiO_2, the amount of PGME removed per unit area of the catalyst surface showed a different trend. As shown in Fig. 8, the immobilized catalyst was able to remove PGME at the level of 0.65 mg cm^{-2} compared with 0.024 mg cm^{-2} for the suspended catalyst. This indicates a significant underutilization of the catalyst surface for suspended TiO_2.

For the same amount of TiO_2, the suspended form would provide a higher total surface area than the immobilized form. However, the available surface area was not illuminated completely by the UV light. When TiO_2 particles were suspended in water, the solution became opaque; hence, this would hinder the penetration of the UV light deep into the solution. Consequently, only catalyst particles close to the surface of the solution would take part in the photocatalytic reaction. In addition, small TiO_2 particles (4–30 nm) aggregated rapidly in the suspension leading to a lower effective surface area [20]. On the other hand, for the immobilized TiO_2, the catalyst was illuminated completely since the TiO_2-coating layer on the ceramic tile faced the UV light. In addition, immobilized TiO_2 on a substrate eliminated the agglomerate problem [21]. Moreover, the electron-hole recombination on the surface of TiO_2 particles would be reduced when TiO_2 is immobilized. All those factors would enhance the efficiency of the photocatalytic reaction [22].

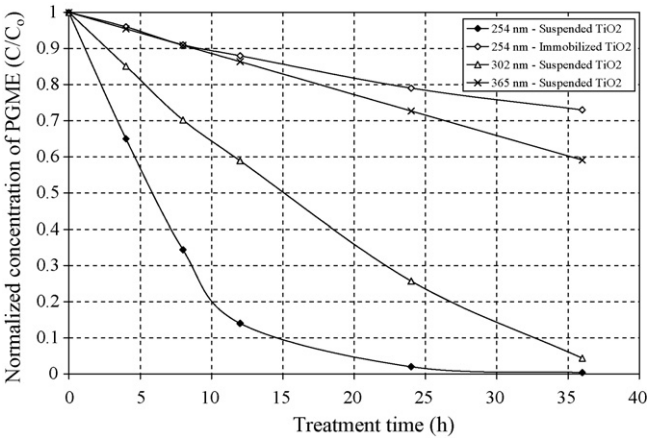

Fig. 7. Effect of UV wavelength on PGME removal with suspended TiO_2 in a batch system, $[PGME]_0 = 200$ ppm, $T = 25\,^{\circ}C$.

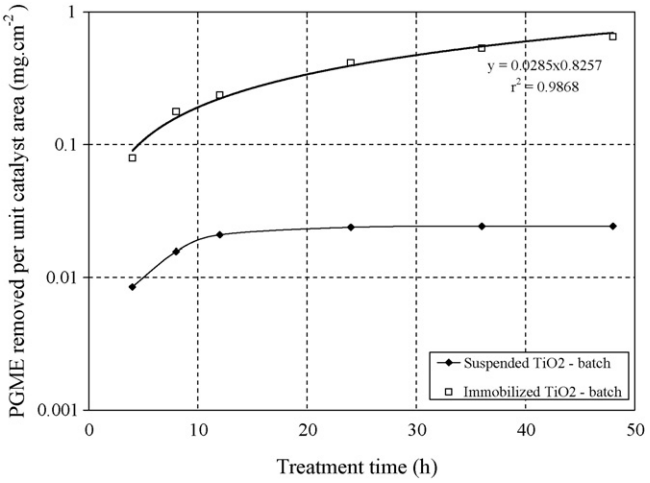

Fig. 8. Amount of PGME removed per unit surface area of suspended and immobilized TiO_2 in a batch system.

3.2.2. Effect of curing time and temperature used in the immobilization of TiO_2

The curing temperature used in the TiO_2 immobilization process may have a significant effect on the activity of the immobilized TiO_2 film. It was reported that in the sol–gel immobilization of P25 TiO_2 at 100 °C for 3 h and then at 500 °C for 1 h, some TiO_2 converted from its original anatase to rutile form. The irreversible transformation of anatase to rutile was more noticeable at 700 °C. Rutile is thermodynamically stable; however, it is less photocatalytically active than anatase [23].

In order to investigate the effect of the curing temperature on the activity of the immobilized TiO_2 film, varied curing temperatures from 25 to 650 °C were tested. After coating TiO_2 on a ceramic tile, the TiO_2 film was allowed to dry at room temperature for 24 h. The TiO_2 coated ceramic tile was then cured at a predetermined temperature for 5 h. The cured TiO_2 coated ceramic tile was finally used in a batch photocatalytic experiment to remove PGME. The experimental data obtained are plotted in Fig. 9. The highest percentage PGME removal was obtained at the curing temperature of 600 °C. Further increase in the curing temperature to 650 °C did not have any significant effect on the removal of PGME. At low temperatures (25, 150 and 300 °C), TiO_2 might be cured only partially for a good bonding of TiO_2 particles to the ceramic support. As a result, TiO_2 particles were detached from the immobilized film and lost to the liquid when the TiO_2 coated ceramic tile was rinsed with water after curing and exposed to moving liquid during the experiments.

The effect of the curing time on the removal of PGME was also examined using varied curing times of 5, 24 and 48 h at 600 °C. The results showed that prolonging the curing time to more than 5 h did not have any significant effect on the removal of PGME as can be seen in Fig. 10. This indicated that the curing duration of 5 h at 600 °C was adequate for the TiO_2 coating on the ceramic support to be dried up and bonded to the support well. Once the TiO_2 film

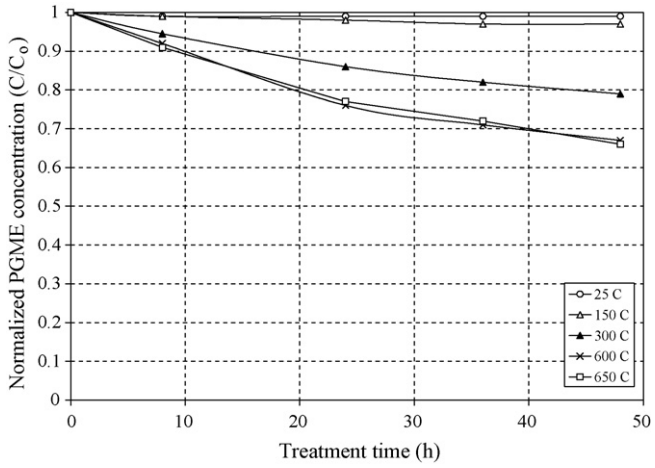

Fig. 9. Effect of curing temperature of TiO_2 immobilized film on the reduction of PGME; $T = 25\,^{\circ}C$, UV 254 nm, $[PGME]_0 = 200$ ppm in batch system.

had been set on the support, further drying had little effect on the film.

3.3. Sole photocatalytic treatment

In order to determine the amount of PGME or metal ions would be physically adsorbed on the surface of TiO_2 or the experimental apparatus, a dark experiment was conducted in the rotary reactor as shown in Fig. 2. A solution of 200 ppm PGME and 20 ppm each of Ni^{2+} and Zn^{2+} was circulated in the system without the UV lamp for 48 h at a volumetric liquid flux of 0.0148 $m^3\,m^{-2}\,s^{-1}$. Physical adsorption of about 7% of PGME on the TiO_2 and the experimental apparatus was observed. This occurred mainly in the first hour. Similarly, the concentrations of Ni^{2+} and Zn^{2+} decreased about 10%. As a result, in order to exclude the reduction of PGME, Ni^{2+} and Zn^{2+} due to physical adsorption, the solution of PGME and metal ions was circulated through the system for 1 h before starting photocatalytic or combined photo-electrochemical experiments.

The effect of the volumetric liquid flux in the rotary reactor on the degradation of PGME was also examined. Liquid volumetric fluxes of 0.0105 and 0.0148 $m^3\,m^{-2}\,s^{-1}$ were used. The results obtained showed that the removal of PGME appeared to be independent of the liquid flux. The rotating motion of the disks in the photocatalytic section of the reactor created radial fluid motion that

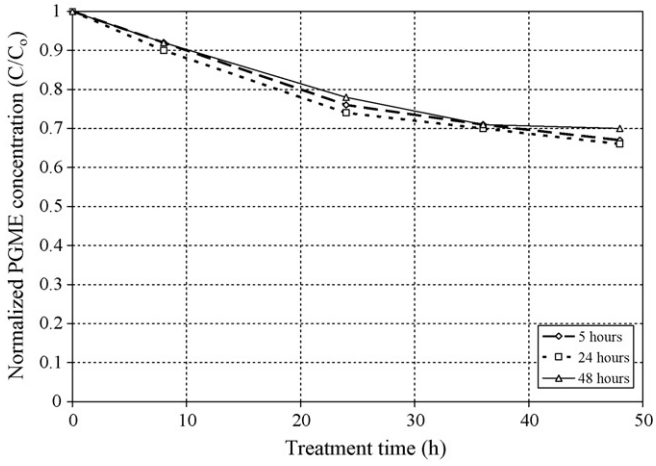

Fig. 10. Effect of annealing time of TiO_2 immobilized film on the reduction of PGME; $T = 25\,^{\circ}C$, UV 254 nm, $[PGME]_0 = 200$ ppm in batch system.

was much higher than the linear fluid velocity. This was indeed the case since the disks rotated at 10 rpm. The equivalent peripheral (linear) velocity of the TiO_2 coated ceramic tiles was 13.2 $cm\,s^{-1}$ while the linear velocity of liquid in the axial direction was varied between 1.05 and 1.48 $cm\,s^{-1}$. Therefore, the mass transfer rate of PGME from the bulk liquid to TiO_2 on the ceramic tiles was mainly influenced by the rotating speed of the disks. The rotational speed of the disks may have some effect of the removal of PGME. This would be an interesting aspect for further study. In the present study, the main objective was to evaluate the capability of a combined electrochemical and photocatalytic method using the immobilized TiO_2 on ceramic tiles; hence, only one rotational speed was used and the effect of the rotational speed on the removal of PGME was not investigated.

3.4. Combined electrochemical and photocatalytic process

The effectiveness of the combined electrochemical and photocatalytic process in treating wastewater containing both metal ions and organic pollutants in a rotary reactor was assessed. A solution containing 20 ppm each of Ni^{2+} and Zn^{2+}, and 200 ppm of PGME was used as a model solution that represented the wastewater from the metal finishing industry.

After 48 h of treatment at a liquid flux of 0.0148 $m^3\,m^{-2}\,s^{-1}$, the concentrations of Ni^{2+} and Zn^{2+} were reduced by 33% and 37%, respectively. The lower percentage metal removal than that of the sole electrochemical treatment can be attributed to a much larger liquid volume used in the combined method. The liquid volume used in the rotary reactor was 2.4 times that used in the sole electrochemical experiment. When the liquid volume was accounted for, the amount of metal removed in the rotary reactor was comparable to that in the sole electrochemical treatment.

Moreover, the presence of anions in the solution may affect the effectiveness of the photocatalytic degradation of the organic compound. The anions might compete with the organic compound for the adsorption sites on the surface of TiO_2 where the degradation of the organic compound occurred. The anions could also react with hydroxyl radicals that were meant for the oxidation of the organic compound. Also, the anions might absorb UV light that was needed for the excitation of TiO_2 to produce hydroxyl radicals. Many researchers have studied the effect of several anions on photocatalytic oxidation of organics. In general, anions such as CO_3^{2-} and HCO_3^- could act as radical scavengers and also affect the adsorption of the organics on TiO_2 surface while Cl^- affected the adsorption strongly and also absorbed UV light. Other anions such as sulfate (SO_4^{2-}), phosphate (PO_4^{3-}) and nitrate (NO_3^-) affected the degradation efficiency marginally [24–27]. It has also reported that the effect of SO_4^{2-}, CO_3^{2-}, Cl^-, and HCO_3^- on the organic degradation could be ranked in the order $SO_4^{2-} < CO_3^{2-} < Cl^- < HCO_3^-$ [28]. In the present study, the presence of SO_4^{2-} and the supporting electrolyte, K_2SO_4, indeed did not affect the removal of PGME significantly.

A comparison of the amount of PGME removed by the combined method with the sole electrochemical and sole photocatalytic techniques in the rotary reactor using the TiO_2 coated ceramic tiles is presented in Fig. 11. It can be seen clearly that the combined method yielded a substantially higher PGME removal as compared to those for the other two methods.

Although almost all of PGME was degraded by suspended TiO_2 in the batch system, this did not show the true efficiency of the suspended system, because of the small liquid volume (1 L) used in the batch experiment. The amount of PGME removed by suspended TiO_2 was 200 mg. For the immobilized TiO_2 on a ceramic tile in a batch experiment, a 33% PGME degradation was observed, which was equivalent to the removal of 66 mg PGME. For the sole photocatalytic process with immobilized TiO_2 in the rotary reactor,

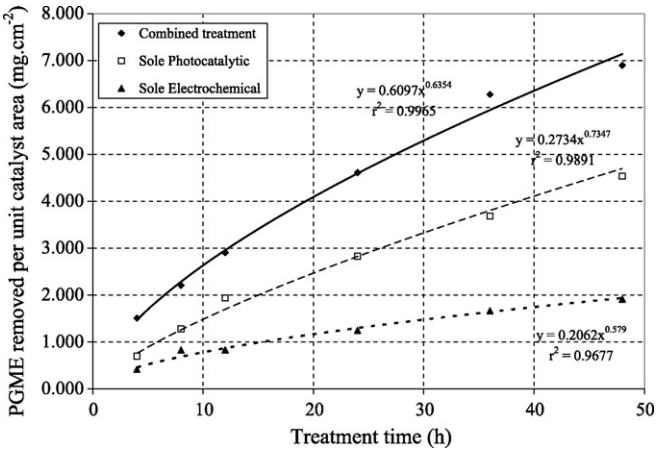

Fig. 11. Comparison of the PGME removal by photocatalytic, electrochemical and combined treatments in a rotary reactor, $T = 25\,^{\circ}C$, liquid flux = 0.0148 $m^3\,m^{-2}\,s^{-1}$.

the PGME removal was only 12%. However, this was equivalent to about 2800 mg PGME removed. When the amount PGME removed per unit area of the catalyst surface was used as the basis for comparison, the immobilized catalyst in the rotary reactor was able to remove 4.6 mg PGME cm^{-2} followed by the batch immobilized catalyst system and the suspended catalyst at 0.65 and 0.024 mg PGME cm^{-2} TiO_2, respectively. By increasing the number of the TiO_2 coated tiles in the rotary reactor, a higher ratio of the immobilized TiO_2 surface area to the volume of wastewater can be realized for a better percentage removal of PGME.

4. Conclusions

In the sole electrochemical treatment with flat plate electrodes, the removal of Ni^{2+} and Zn^{2+} was almost doubled when the electrode spacing was decreased from 6.4 to 1.3 cm. In addition, the corrugated cathode led to a further 40% increase in the amount of metal ions removed. With the corrugated electrodes at the spacing of 1.3 cm, a 96% removal each for both Ni^{2+} and Zn^{2+} was achieved after 48 h of treatment.

For the sole photocatalytic treatment in a batch system, suspended TiO_2 in the wastewater could remove PGME almost completely after 48 h of treatment while the immobilized TiO_2 film on a ceramic tile support was only able to remove 33% of PGME. However, based the surface area of the catalyst, the immobilized TiO_2 gave a better PGME removal of 0.65 mg cm^{-2} as compared with 0.024 mg cm^{-2} for the suspended TiO_2.

In the TiO_2 immobilization process, the curing temperature affected the efficiency of the TiO_2 film significantly. Over the curing temperature range of 25–650 °C, the best performance was obtained with the immobilized film cured at 600 °C. On the other hand, the curing time of 5 h was found to be adequate. Prolonged curing time up to 48 h did not have any significant effect on the performance of the TiO_2 film.

Using the TiO_2 immobilization technique developed in the present study, a long lasting and active TiO_2 film was successfully bonded to the ceramic tile support. The combined electrochemical and photocatalytic process in a rotary reactor improved the removal of PGME significantly over the sole photocatalytic or sole electrochemical treatment. Moreover, Ni^{2+} and Zn^{2+} were also removed concurrently in the combined system. The combined process could thus be considered as a good alternative method for the treatment wastewater containing both organic and heavy metal pollutants.

Acknowledgement

Financial support from the National Science and Engineering Research Council of Canada (NSERC) to this project is greatly appreciated.

References

[1] L. Feigelson, L. Muszkat, L. Bir, K.A. Muszkat, Dye photo-enhancement of TiO_2-photocatalyzed degradation of organic pollutants: the organobromine herbicide bromacil, Water Science Technology 42 (2000) 275–279.
[2] E. Otal, D. Mantzavinos, M.V. Delgado, R. Hellenbrand, J. Lebrato, I.S. Metcalfe, A.G. Livingston, Integrated wet air oxidation and biological treatment of polyethylene glycol containing wastewaters, Journal of Chemical Technology and Biotechnology 70 (1997) 147–156.
[3] D. Mantzavinos, R. Hellenbrand, A.G. Livingston, I.S. Metcalfe, Reaction mechanisms and kinetics of chemical pretreatment of bioresistant organic molecules by wet air oxidation, Water Science and Technology 35 (4) (1997) 119–127.
[4] H. Doan, J. Wu, Biological treatment of wastewater from polymer coating process, Journal of Chemical Technology and Biotechnology 77 (2002) 1076–1083.
[5] K. Rajeshwar, J.G. Ibanez, Environmental Electrochemistry Fundamentals and Application in Pollution Abatement, Academic Press, New York, 1997.
[6] G. Orhan, C. Arslan, H. Bombach, M. Stelter, Nickel recovery from the rinse water of plating baths, Hydrometallurgy 65 (2002) 1–8.
[7] G. Prentice, Electrochemical Engineering Principles, Prentice-Hall International, Englewood Cliffs, NJ, 1991.
[8] D. Pletcher, F. Walsh, Industrial Electrochemistry, 2nd edition, Chapman-Hall, London, 1990.
[9] K.E.M. Scott, E.M. Patton, An analysis of metal recovery by electrodeposition from mixed metal ion solutions. Part I. Theoretical behavior of batch recycle operation, Electrochimica Acta 38 (1993) 2181–2189.
[10] A. Brenner, Electrodeposition of Alloys. Principles and Practice, vol. 1 and 2, Academic Press, New York, 1963.
[11] D.J. Pickett, Electrochemical Reactor Design, 2nd edition, Elsevier Scientific Publishing Company, New York, 1979.
[12] C.E. Lehmberg, D.B. Lewis, G.W. Marshall, Composition and structure of thin electrodeposited zinc–nickel coatings, Surface and Coating Technology 192 (2005) 269–277.
[13] R. Fratesi, G. Roventi, Electrodeposition of zinc–nickel alloy coating from a chloride bath containing NH_4Cl, Journal of Applied Electrochemistry 22 (1992) 657–662.
[14] G. Roventi, R. Fratesi, R.A. Della Guardia, G. Barucca, Normal and anomalous codeposition of Zn–Ni alloys from chloride bath, Journal of Applied Electrochemistry 30 (2000) 173–179.
[15] N. Tzanetakis, K. Scott, W.M. Taama, R.J.J. Jachuck, Mass transfer characteristics of corrugated surfaces, Applied Thermal Engineering 24 (2004) 1865–1875.
[16] R.B. Bird, W.E. Stewart, E.N. Lightfoot, Transport Phenomena, 2nd edition, John Wiley & Sons, Inc., New York, 2002.
[17] A. Anderko, M.M. Lenka, Modeling self-diffusion in multicomponent aqueous electrolyte systems in wide concentration ranges, Industrial Engineering Chemistry Research 37 (1998) 2878–2888.
[18] J.R. Welty, C.E. Wicks, R.E. Wilson, G. Rorrer, Fundamentals of Momentum, Heat, and Mass Transfer, 4th edition, John Wiley & Sons, Inc., New York, 2001.
[19] H.D. Doan, M. Saidi, Simultaneous removal of metal ions and linear alkylbenzene sulfonate by a combined electrochemical and photocatalytic process, Journal of Hazardous Materials 158 (2008) 557–567.
[20] A. Bhattacharyya, S. Kawi, M.B. Ray, Photocatalytic degradation of orange II by TiO_2 catalyst supported on adsorbents, Catalysis Today 98 (2004) 431–439.
[21] Y. Xu, C.H. Langford, Enhanced photoactivity of titanium (IV) oxide supported on ZSM5 and Zeolite A at low coverage, Journal of Physical Chemistry 99 (1995) 11501–11507.
[22] C. Anderson, A.J. Bard, An improved photocatalyst of TiO_2/SiO_2 prepared by a sol–gel synthesis, Journal of Physical Chemistry 99 (1995) 9882–9885.
[23] M. Bideau, B. Claudel, C. Dubien, L. Faure, H. Kazouan, On the "immobilization" of titanium dioxide in the photocatalytic oxidation of spent waters, Journal of Photochemistry and Photobiology A: Chemistry 91 (1995) 137–144.
[24] M. Abdullah, G.K.C. Low, R.W. Matthews, Effects of common inorganic anions on rates of photocatalytic oxidation of organic hydrocarbons over illuminated titanium dioxide, Journal of Physical Chemistry 94 (1990) 6620.
[25] T.Y. Wei, Y.Y. Wang, C.C. Wan, Photocatalytic oxidation of phenol in the presence of hydrogen peroxide and TiO_2 powder, Journal of Photochemistry and Photobiology 55 (1990) 115–126.
[26] C. Kormann, D.W. Bahnemann, M.R. Hoffmann, Photolysis of chloroform and other organic molecules in aqueous TiO_2 suspensions, Environment Science Technology 25 (1991) 494–500.
[27] E.C. Butler, A.P. Davis, Photocatalytic oxidation in aqueous titanium dioxide suspensions: the influence of dissolved transition metals, Journal of Photochemistry and Photobiology 70 (1993) 273–283.
[28] A.A. Yawalkar, D.S. Bhatkhande, V.G. Pangarkar, A.A.C.M. Beenackers, Solar assisted photochemical and photocatalytic degradation of phenol, Journal of Chemical Technology and Biotechnology 76 (2001) 363–370.